Gravitational Effects on Near Field Flow Structure of Low Density Gas Jets

Tze-Wing Yep and Ajay K. Agrawal[1]
School of Aerospace and Mechanical Engineering
University of Oklahoma, Norman, OK 73019

DeVon Griffin
Microgravity Science Division
NASA Glenn Research Center
Cleveland, OH

ABSTRACT

Experiments were conducted in Earth gravity and microgravity to acquire quantitative data on near field flow structure of helium jets injected into air. Microgravity conditions were simulated in the 2.2-second drop tower at NASA Glenn Research Center. The jet flow was observed by quantitative rainbow schlieren deflectometry, a non-intrusive line of site measurement technique for the whole field. The flow structure was characterized by distributions of angular deflection and helium mole percentage obtained from color schlieren images taken at 60 Hz. Results show that the jet flow was significantly influenced by the gravity. The jet in microgravity was up to 70 percent wider than that in Earth gravity. The jet flow oscillations observed in Earth gravity were absent in microgravity, providing direct experimental evidence that the flow instability in the low-density jet was buoyancy induced. The paper provides quantitative details of temporal flow evolution as the experiment undergoes a change in gravity in the drop tower.

[1] Corresponding Author, Member AIAA
865 Asp Avenue, Room 212
School of Aerospace and Mechanical Engineering
University of Oklahoma, Norman, OK 73019

Introduction

Low-density jets are found in many engineering applications and natural phenomena, for example, exhaust from engines and stacks in industry, fuel leaks and accidental fires, diffusion flames, and geophysical events such as volcanic eruptions. Several recent studies [1-3] have focused on the far-field behavior of low-density jets using helium as the jet fluid. However, the near field jet behavior has direct influence on the acoustic noise and flow development in the far field. Thus, an understanding of the flow structure in the near field of low-density gas jets is of significant fundamental importance. Subbarao and Cantwell [4] studied the near field flow behavior of vertical helium jets issued from a tube into a co-flow of air. The jets were characterized as buoyant for jet Richardson number, $Ri = [gd(\rho_a-\rho_j)/ \rho_j U_j^2$ where g is the gravitational acceleration, d is the tube inside diameter, ρ_a and ρ_j are, respectively, the free-stream and jet densities, and U_j is the mass-averaged jet exit velocity] varying between 0.5 and 6.0. They observed an extremely regular flow field consisting of periodic formation and breakdown of helium-containing vortical cells. Measurements revealed large centerline velocity fluctuations, and early and abrupt breakdown of the potential core. Even the large-scale structure after the breakdown repeated itself with regularity. The Strouhal number, $St =[f\ d/U_j$ where f is the oscillation frequency] of the oscillating mode was independent of the Reynolds number. For $Ri < 0.50$, the Strouhal number was also independent of the Richardson number. However, for $Ri > 1.0$, St scaled with Ri, indicating the presence of a buoyancy-dependent instability mode. They speculated that the perturbation in the air stream, for

Phone: (405)325-1754, fax: (405) 325-1088, email: aagrawal@ou.edu

example, on the surface boundary layer outside the jet tube, were likely to dominate the flow instability and transition processes.

Pulsations in the near field of helium jets flowing into quiescent air were also observed by Hamins et al [5], who found that a minimum jet velocity was required to trigger the oscillations. The measured St correlated with the Richardson number (i.e., the inverse Froud number), demonstrating that the oscillations were buoyancy induced. They found that the St-Ri correlation for helium jets differed from that found for flickering flames, implying differences in the buoyancy effects in non-reacting and reacting jets. Experiments in naturally unstable helium jets by Cetegen and Kasper [6] extended the operating regime of Richardson numbers to those in pool fires and buoyant plumes. The oscillation frequency was represented by correlation between St and Ri for Ri varying from 1.5 to 5.0×10^{4}. Phase resolved laser Doppler velocity measurements revealed a toroidal vortex ring forming near the jet exit because of the buoyant acceleration of the jet fluid accompanied with strong radial inflow of the surrounding fluid. The toroidal vortex was initially located in the region of the highest centerline velocity. Subsequently, the flow field was determined by the toroidal vortex as it convected downstream. Similar mechanistic details of vortex formation and convection were reported by Cetegen [7] using particle image velocimetry.

In the studies reported above, the Richardson number was close to or above unity, and hence, the jets were characterized as buoyant. Flow oscillations in the near-field of low density jets have also been observed in momentum-dominated jets at Richardson numbers below $1.x10^{-3}$ [8-10]. In addition, the experiments by Richards et al [11] represent the range between the buoyant jets of Subbarao and Cantwell [4] and the

momentum-dominated jets of Kyle and Sreenivasan [10]. These studies show striking similarity in the near field flow behavior of low-density gas jets in flow regimes varying from buoyancy-dominated to momentum-dominated.

Although the near field oscillations in gas jets at high Richardson numbers are attributed to the buoyancy, direct physical evidence has not been acquired in experiments. If the instability was indeed caused by buoyancy, the near-field flow structure of the jet would undergo significant changes upon removing buoyancy, for example, in the microgravity environment. The present study was conducted to investigate this effect in low-density gas jets considered buoyant in Earth gravity. The flow structure was quantified by measurements using the quantitative Rainbow Schlieren Deflectometry (or RSD) technique [12]. The RSD is a non-intrusive optical diagnostics technique to measure scalar quantities across the whole field at high spatial and temporal resolutions. The technique was demonstrated previously for measurements of concentration profiles in helium jets [13, 14], and temperature field in diffusion flames [15-17] and partially premixed flames [18]. The microgravity environment was simulated in the 2.2-second drop tower facility at the NASA Glenn Research Center. Results are presented for a steady jet and an unsteady jet in Earth gravity to highlight significant gravitational effects on the flow structure. The experimental approach, results and conclusions of the study are presented in the following sections.

Experimental Approach

The experimental setup is housed in a drop rig, 840-mm high, 960-mm long and 400-mm wide, with a standard aluminum A-frame. Al-Ammar [17], who conducted

experiments with hydrogen gas-jet diffusion flames in Earth and microgravity, completed the initial setup. The experimental setup was modified to perform helium jet experiments for the present study. It consists of three major components: flow system, rainbow schlieren apparatus, and image recording system.

Figure 1 shows a schematic of the flow system. Helium gas was supplied from two 1000 cm^3 pressurized cylinders. A pressure relief valve set to 1.38 MPa (200 psig) was placed between the cylinders. The pressure regulator maintained the gas supply pressure at 690 kPa (100 psig). A calibrated mass flow meter was used to measure the helium gas flow rate. The gas flow rate was controlled by a metering valve. A solenoid valve was used to instantaneously activate or block the gas flow. A positioning jack was used to locate the jet tube exit with respect to the schlieren field of view. Jet tubes of 19mm and 32mm inside diameter were used in this study. The upstream and bend regions of the jet tube were filled with steel wool to minimize the flow non-uniformities. Steel screens were placed at the inlet and exit sections of the bend region. Figure 2 shows geometric details of a jet tube used in this study. The straight length of jet tube was limited to about 0.30m because of the spatial constraints of the drop rig.

The jet flow structure was visualized and quantified by the rainbow schlieren apparatus depicted in Figure 3. The light input to a 5-μm wide and 3-mm high source aperture is provided by a 150-W halogen light source connected through a 600-μm diameter fiber-optic cable. The source aperture is placed at the focal point of an 80-mm diameter, 310-mm focal length collimating lens. The collimated light rays passing through the test section are deflected because of density gradients in flow field. Then the light rays are decollimated by an 80-mm diameter, 1000-mm focal length decollimating

lens. Because of the space constraints of the setup, a pair of 100-mm diameter, aluminum coated flat surface mirrors were used to fold the rays by 180 degrees. The folded light rays form the displaced image of the source aperture on a 3.5-mm wide, computer generated, symmetric, rainbow filter. The rainbow filter is placed at the focal point of the decollimating lens. A camera lens of 75-mm focal length is used to image the test section onto the CCD array. Schlieren images were acquired by the color camera at 60 field images per second, and digitized by a 24-bit color frame grabber installed in the on-board computer. Images were stored in TIFF format at pixel resolution of 640x480.

The test sequence was automated by data acquisition and control systems resident on the computer. First, the computer fans were turned off to minimize flow disturbances. Then, the solenoid valve was activated to turn on the jet flow. After the flow reached steady state, the frame grabber was initiated to acquire the color schlieren images. Next, the experiment was released to simulate microgravity conditions in the drop tower. After the impact, the computer fans were turned on and the gas supply was cut off. After retrieving the drop rig, the image data were transferred from computer memory to an external data-storage device. For each experiment, the schlieren images were acquired for about 1 second in Earth gravity and 2 seconds in microgravity.

Schlieren Analysis

The angular deflection of a light ray by an axisymmetric refractive index field is given for small deflections by the following relationship:

$$\varepsilon(y) = 2y\int_{y}^{\infty} \frac{d\delta}{dr}\frac{dr}{\sqrt{\left(r^2 - y^2\right)}}, \qquad (1)$$

where $\delta = (\eta\text{-}1)$ is the refractive index difference, and η is the refractive index of the test medium normalized by that of the surrounding air. In the RSD technique, the deflection angle is determined from measurements of color (or hue) in the schlieren image and the color filter calibration curve [13]. The refractive index difference is obtained by Abel inversion of Eq. (1) expressed in discrete form as

$$\delta(r_i) = \delta(i.\Delta r) = \sum_{j=i}^{NN} D_{ij}.\varepsilon_j, \tag{2}$$

where Δr is the sampling interval and D_{ij} are geometric coefficients given by [19]. For an ideal gas at constant temperature (T) and pressure (P), the refractive index difference is:

$$\delta = \frac{P}{\bar{R}T}\sum_l \kappa_l X_l M_l, \tag{3}$$

where $\bar{R}$ is the universal gas constant, κ is the Dale-Gladstone constant, X is the species mole percentage, and M is the species molecular weight. The summation in Eq. 3 is taken over three species, i.e., oxygen, nitrogen, and helium. Equation 3 was used to construct a table between δ and helium mole percentage, assuming nitrogen to oxygen mole ratio of 3.76 in air.

Results and Discussion

Several experiments were conducted in the drop tower using tubes with d=19.05mm and 31.75mm. Flow characteristics are presented next for a jet that was steady and a jet that was oscillating in Earth gravity. In Table 1, the jet exit Reynolds number is defined as $Re = \rho_j.U_j.d/\mu$, where μ is the dynamic viscosity of helium.

Steady Jet

Figure 4(a) and 4(b) show, respectively, the contours of angular deflection and helium mole percentage in Earth gravity. The radial and axial coordinates are normalized by the tube inside diameter. The contour plots are shown only for the right side of the jet because of the symmetry. The jet boundary represented by zero angular deflection is outside the contour level '1' (i.e., ε=0.0002 radian) in Fig. 4(a). Results show that the jet diffuses radially to r/d>0.7 near the tube exit. Subsequently, the jet width remains nearly constant in the flow direction. Evidently, the radial spread of the jet shear layer between helium and air was countered by the buoyant acceleration of the core region. In Fig. 4(b), the angular deflection near the jet exit region up to z/d=1.0 is higher than that in the downstream region. This is explained by the higher concentration gradients near the jet exit as shown in Figure 5. Evidently, the helium concentration in the center region decreased in the axial direction even though the jet did grow radially. Figure 5 suggests that the flow in the core region accelerates to satisfy the mass conservation of helium issuing from the jet.

The evolution of the jet as it undergoes microgravity conditions in the drop tower is shown by a sequence of contour plots of angular deflection and helium mole percentage, shown respectively, in Figure 6 and 7. With change from Earth gravity to microgravity, the jet widens instantly at the exit region, where steady conditions are reached within 1/5s (see Fig. 6c and 7c). The flow continues to evolve in the axial direction as the jet widens throughout the field-of-view. The jet width in microgravity is higher than that in Earth gravity by 35 percent at z/d=0.3 and 70 percent at z/d=3.0. Figure 7(f) shows helium contour lines diverging away from the center, signifying a typical shear layer of a non-

buoyant jet. In contrast, the helium contour lines in Earth gravity (Fig. 7a) converge towards the center because of the flow acceleration as explained above in the context of Fig. 5. Figure 8 shows comparison of radial profiles of helium mole percentage in Earth and microgravity at z/d=1.5. Because of the lack of buoyancy in microgravity, the helium diffuses further into air. In this case, the jet width in microgravity is about 65 percent higher than that in Earth gravity.

Previous flow studies in drop towers have raised concerns about achieving steady microgravity conditions within the limited duration of the drop. To examine this issue, we show time traces of angular deflection and helium mole percentage at z/d=1.5, respectively, in Fig. 9(a) and 9(b). In these figures, the time, t=0 represents start of the drop. Results show that with change in gravity, the jet initially spreads radially to a peak location and thereafter, it contracts slightly before reaching steady conditions. The radial peak occurs later in the outer region of the jet, suggesting that the jet interior flow responds more quickly to the change in gravity. According to Figure 9(b), the time delay between radial peak locations of 50% and 10% helium mole percentage profiles is about 0.08s. The jet expands until about t=0.62s and steady conditions are reached throughout the jet after about t=1.0s. These results show that the 2.2s duration of the drop was adequate for the experiment.

Oscillating Jet

At Re=300 and Ri=1.44, corresponding to the second case in Table 1, the jet exhibited periodic oscillations of the flow field. Figure 10 shows contour plots of the helium mole percentage obtained from a sequence of schlieren images to depict an

oscillation cycle. Each contour plot is $1/60^{th}$ of a second apart. The field-of-view in the axial direction was limited to z/d=1.6 because of the larger tube diameter (d=31.75mm). Results show that the helium mole percentage varied throughout the flow field during the oscillation cycle. In Fig. 10(a), the radial inflow of heavier air compresses the jet core region until about z/d=0.35. This process continues in the next Figure 10(b), where the jet compression is observed until about z/d=0.75. A vortex is present in the next plot (Figure 10c), which shows the 50% mole percentage contour at two distinct radial locations near z/d=1.4. Figures 10(b) and 10(c) suggest that the vortex develops between z/d=0.8 and 1.4 although the precise location could not be identified because of the limited temporal resolution of the present imaging system (60Hz). Figures 10(d) and (e) show that the near exit jet region expands as the vortex convects downstream of the field-of-view. The cycle repeats itself with radial inflow of air compressing the jet core region as shown in Fig. 10(f). The contour plot in Fig 10(f) is similar, though not identical, to that in Fig. 10(a) suggesting that the oscillation frequency is approximately 12Hz. This is confirmed by frequency power spectra of angular deflection at several locations shown in Figure 11. The power-spectra reveal a dominant frequency of 12.2 Hz at all locations suggesting a global flicker frequency as discussed by Richards et al [11].

The evolution of the jet flow structure with change in gravity is depicted in Fig. 12 by a sequence of contour plots of helium mole percentage. In Fig. 12(a), the jet is compressed by radial inflow of surrounding air in Earth gravity. A vortex is present at z/d=1.3 immediately after the drop is initiated, as shown in Fig 12(b). At this time, the jet has expanded radially near the exit region. The vortex is still present in Fig. 12(c) at t=2/60s after drop initiation and the jet expansion continues in the exit region.

Subsequently, the jet continues to expand radially even though the vortex has moved away from the view-of-view. Thus, the radial compression of the jet near the exit region and the flow field oscillations are not observed. Similar to Fig. 7(f), the helium mole percentage contours in microgravity are straight lines reminiscent of typical non-buoyant jets. In microgravity, the jet width exceeded the field of view of the schlieren apparatus. In the absence of a reference point in the surrounding medium (air), systematic errors were introduced during the Abel inversion process. This explains the contours lines in Fig. 12(f), which do not diverge as expected in non-buoyant jets. Power spectra of angular deflection were obtained to assess the oscillation characteristics of the jet flow in microgravity. The analysis was performed using 1.1s of data taken in the beginning and towards the end of the drop to distinguish initial transients from steady conditions. Fig. 13 shows oscillations without a distinct frequency when data at the beginning of the drop is used. Data taken at the end of the drop however did not produce any detectable flow oscillations. These results provide direct physical evidence that flow oscillations in the jet were buoyancy induced.

A description of the jet flow during transition from Earth gravity to microgravity is given in Fig. 14 by time traces of helium mole percentage at z/d=1.0. The oscillating jet flow expands in the radial direction as it responds to the change in gravity. Figure 14 shows that the inner jet region expands prior to the outer region. Oscillations are observed in the initial period of microgravity, especially in regions with higher helium mole percentage in Fig. 14. However, both the oscillation frequency and amplitude are small. Results indicate that the jet reaches steady conditions within t=1.0s.

Further understanding of the jet flow during transition from Earth gravity to microgravity is gained from Figure 15 showing helium mole percentage profiles at different axial locations for r/d=0.6. Near the jet exit at z/d=0.5 (Fig. 15a), the helium mole percentage in Earth gravity varied between 10 and 20. As the jet expanded in microgravity, the helium concentration increased to about 90 percent within 0.12s. Thereafter, the flow oscillations continued although both mean and amplitude of concentration decreased with time. Steady conditions were reached in about 1.0s, corresponding to helium mole percentage of about 55. At a downstream location z/d=1.0 (Fig 15b), a peak concentration of 90 percent helium was reached in 0.17s of microgravity. Subsequently, the jet oscillated before reaching steady concentration of 40 percent helium in about 1.0s. Further downstream at z/d=1.5 (Fig. 15c), the helium concentration in Earth gravity varied between 15 and 40 percent. In this case, the peak helium concentration was reached after 0.22s second of microgravity. The jet did not oscillate after about 0.40s and a steady value of 35 percent helium was reached within 0.75s. A comparison of profiles in Fig 15 reveals that the jet oscillations stopped earlier in the downstream region. These results provide direct physical evidence that buoyancy-induced flow oscillations in the low-density gas jet were triggered by instabilities in the downstream region of the jet. These observations substantiate the results obtained Cetegen [20] using helium-gases in Earth gravity.

Conclusions

The non-intrusive, line-of-sight, RSD technique was utilized for quantitative flow measurements in the near field of buoyant and non-buoyant helium gas jets. Results show

that the radial growth of the jet shear layer in Earth gravity is hindered by the buoyant acceleration. The jet core region is however diluted by air as the flow accelerates by buoyancy. The jet in microgravity is 30 to 70 percent wider than that in Earth gravity. The microgravity jet shows typical growth of a non-buoyant jet shear layer. In case of the unsteady jet, the flow oscillations continued as the jet adjusted to the change in gravity. However, the flow oscillations are not present at the end of the drop when steady flow conditions in microgravity are reached. Results provide direct physical evidence, for the first time, that the flow oscillations in low-density jets are buoyancy-induced and that the flow instability originates in the downstream region of the jet. Finally, the rainbow schlieren apparatus was shown to provide quantitative scalar measurements across the whole field in the microgravity environment.

Acknowledgment

This work was support by the NASA grant NAG 3-2388.

REFERENCES

1. So, R.M.C., Zhu, J.Y., Otugen, M.V., and Hwang, B.C., 1990, "Some Measurements in a Binary Gas Jet," *Experiments in Fluids*, vol. 9, pp. 273-284.

2. Richards, C.D., and Pitts, W.M., 1993, "Global Density Effects on the Self Preservation Behaviour of Turbulent Free Jets," *Journal of Fluid Mechanics*, vol. 254, pp. 417-435.

3. Panchapakesan, N.R., and Lumley, J.L., 1993, "Turbulence Measurements in Axisymmetric Jets of Air and Helium. Part 2. Helium Jet," *Journal of Fluid Mechanics*, vol. 246, pp. 225-248.

4. Subbarao, E.R., and Cantwell, B.J. (1992). "Investigation of a Co-Flowing Buoyant Jet: Experiments on the Effect of Reynolds Number and Richardson Number," *Journal of Fluid Mechanics*, vol. 245, pp. 69-90.

5. Hamins, A., Yang, J.C., and Kashiwagi, T. (1992). "An Experimental Investigation of The Pulsating Frequency of Flames," *Proceedings of the Combustion Institute*, vol. 24, pp. 1695-1705.

6. Cetegen, B.M., and Kasper, K.D. (1996). "Experiments on the Oscillatory Behavior of Buoyant Plumes of Helium and Helium-Air Mixtures," *Physics of Fluids*, vol. 8, pp 2974-2984

7. Cetegen, B.M., 1997, "Measurements of Instantaneous Velocity Field of a Non-Reacting Pulsating Buoyant Plume by Particle Image Velocimetry" *Combustion Science and Technology*, vol. 123, pp. 377-387.

8. Monkewitz, P.A., Bechert, D.W., Barsikow, B., and Lehmann, B., 1990, "Self-Excited Oscillations and Mixing in a Heated Round Jet," *Journal of Fluid Mechanics*, vol. 213, pp. 611-639.

9. Screenivasan, K.R., Raghu, S., and Kyle, D. (1989). "Absolute Instability in Variable Density Round Jets," *Experiments in Fluids*, vol. 7, pp. 309-317.

10. Kyle, D.M., and Sreenivasan, K.R., 1993, "The Instability and Breakdown of a Round Variable-Density Jet," *Journal of Fluid Mechanics*, vol. 249, pp. 619-664.

11. Richards, C.D., Breuel, B.D., Clark, R.P., and Troutt, T.R. (1995). "Concentration Measurements in a Self-Excited Jet," *Experiments in Fluids*, vol. 21, pp. 103-109.

12. Greenberg, P.S., Klimek, R.B., and Buchele, D.R. (1995). "Quantitative Rainbow Schlieren Deflectometry," *Applied Optics*, vol. 34, pp. 3819-3822.

13. Al-Ammar, K., Agrawal, A.K., Gollahalli, S.R., and Griffin, D.W. (1998). "Application of Rainbow Schlieren Deflectometry for Concentration Measurements in an Axisymmetric Helium Jet," *Experiments in Fluids*, vol. 25, pp. 89-95.

14. Pasumarthi, K.S. (2000). "Full Field Scalar Measurements in a Pulsating Helium Jet Using Rainbow Schlieren Deflectometry," *M.S. Thesis*, University of Oklahoma.

15. Albers, B.W., and Agrawal, A.K. (1999). "Schlieren Analysis of an Oscillating Gas-Jet Diffusion Flame," *Combustion and Flame*, vol. 119, pp. 89-94.

16. Shenoy, A.K., Agrawal, A.K., and Gollahalli, S.R. (1998). "Quantitative Evaluation of Flow Computations by Rainbow Schlieren Deflectometry," *AIAA Journal*, vol. 36, pp. 1953-1960

17. Al-Ammar, K., Agrawal A.K., and Gollahalli, S.R. (2000). "Quantitative Measurements of Laminar Hydrogen Gas-Jet Diffusion Flames in a 2.2 s Drop Tower," *Proceedings of the Combustion Institute*, vol. 28, pp. 1997-2004.

18. Xiao, X., Puri, I.K., and Agrawal, A.K., "Temperature Measurements in Steady Axisymmetric Partially Premixed Flames using Rainbow Schlieren Deflectometry," in print, *Applied Optics*.

19. Agrawal, A.K., and Albers, A.K., 1999, "Abel Inversion of Deflectometric Measurements in Dynamic Flows," *Applied Optics*, vol. 38, pp. 3394-3398.

20. Cetezen, B., 1997, "Behavior of Naturally Unstable and Periodically Forced Axisymmetric Buoyant Plumes of Helium and Helium-Air Mixtures," *Physics of Fluids*, vol. 9, No. 12, pp. 1-11.

TABLE 1

Summary of Test Conditions

Case	d, mm	U_j, m/s	Re	Ri	f, Hz
Test 1	19.05	1.54	240	0.49	Non-oscillating
Test 2	31.75	1.15	300	1.44	12.2

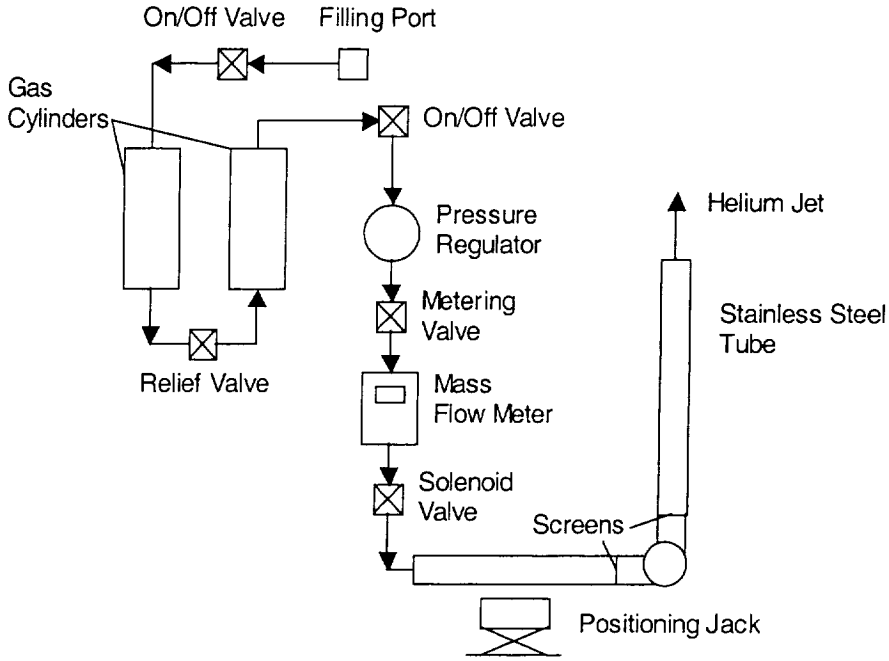

FIG. 1. Schematic diagram of the flow system.

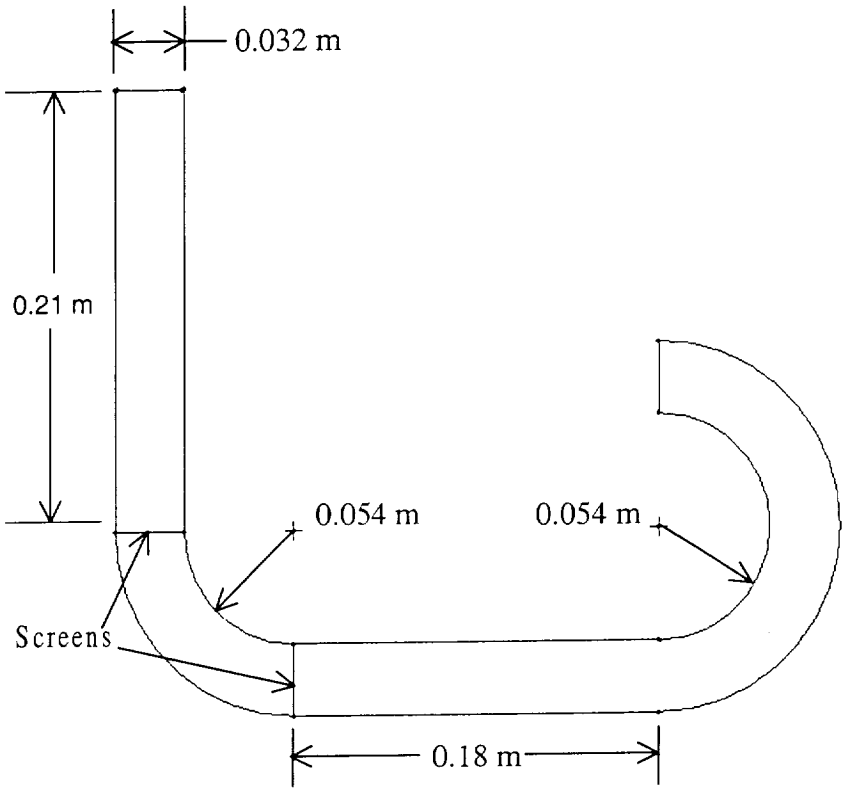

FIG. 2. Geometry of the jet tube (d = 31.75 mm).

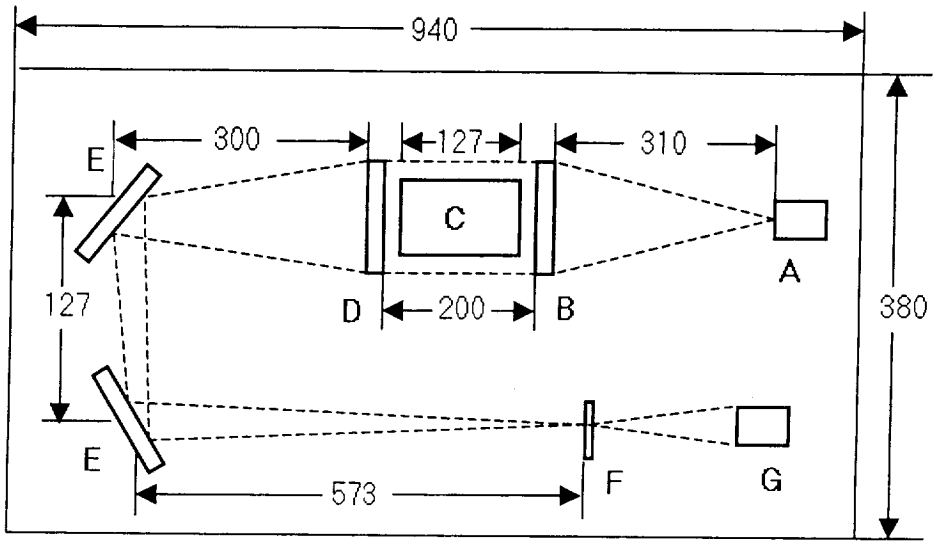

FIG. 3. Optical layout of the rainbow schlieren apparatus (all dimensions are in mm). A: Source Aperture; B: Collimating lens; C: Test Medium; D: Decollimating lens; E: Flat Surface Mirrors; F: Color Filter; G: CCD Array with lens

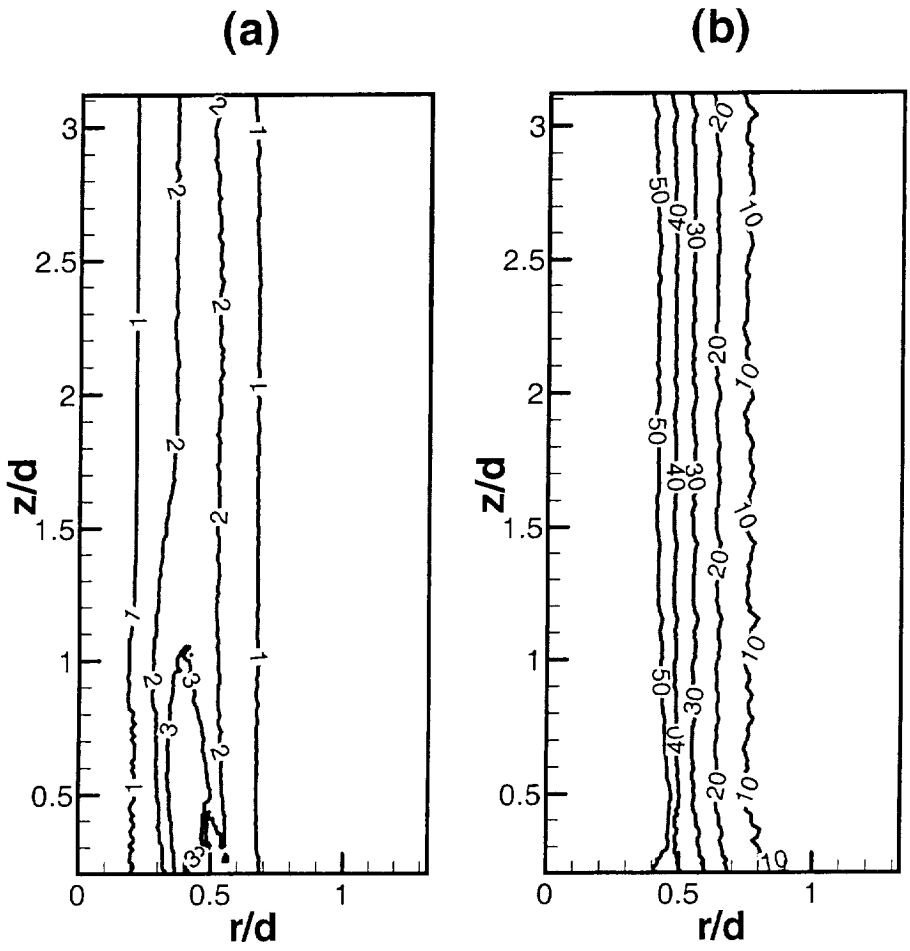

FIG. 4. Contours in Earth gravity: (a) angular deflection; contour labels are 1:0.0002, 2:0.0004, and 3:0.0006 radians; (b) helium mole percentage.

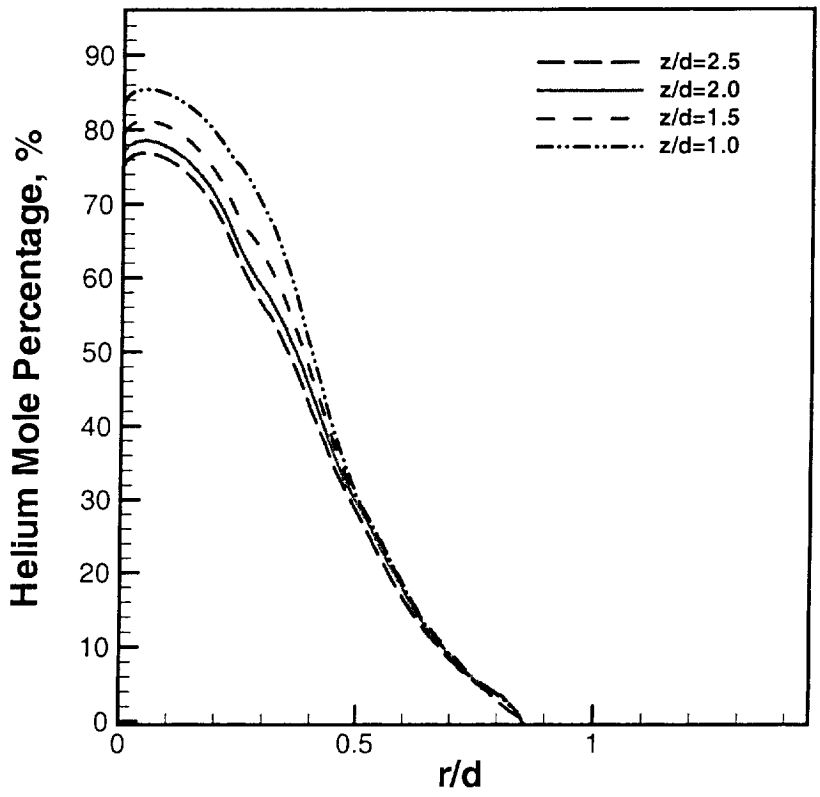

FIG. 5. Helium mole percentage in Earth gravity at various axial locations.

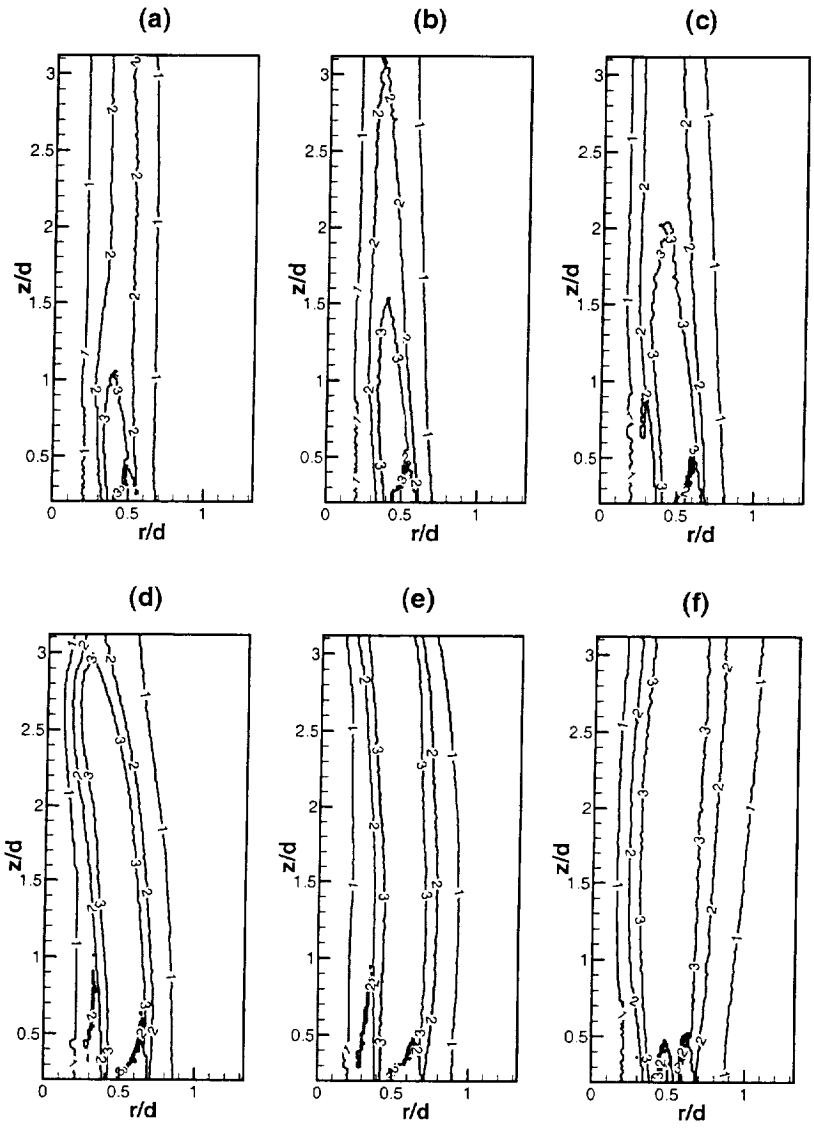

FIG. 6. Contours of angular deflection at: (a) t = 0 sec, (b) t = 1/30 sec, (c) t = 3/30 sec, (d) t = 6/30 sec, (e) t = 10/30, and (f) t = 2.0 sec. Contour labels are 1:0.0002, 2:0.0004, and 3:0.0006 radians.

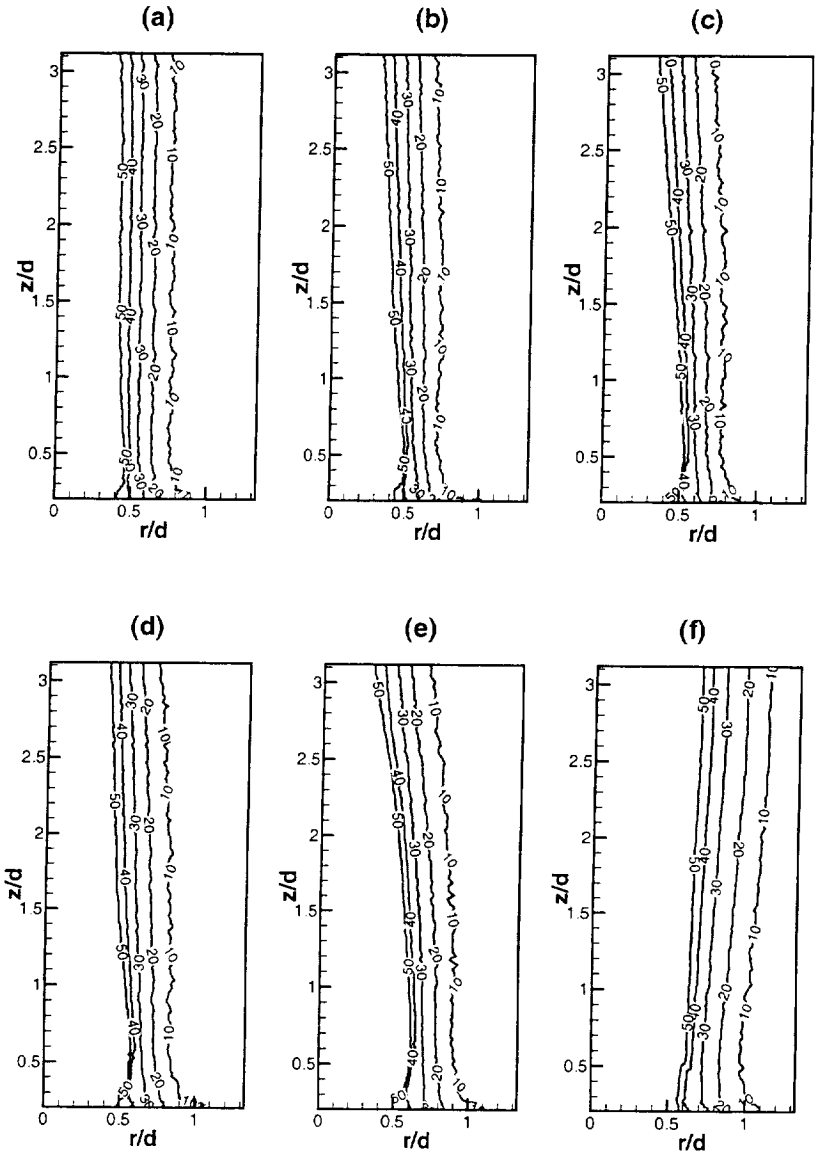

FIG. 7. Contours of helium mole percentage at: (a) t = 0 sec, (b) t = 1/30 sec, (c) t = 2/30 sec, (d) t= 3/30 sec, (e) t = 6/30, and (f) t = 2.0 sec.

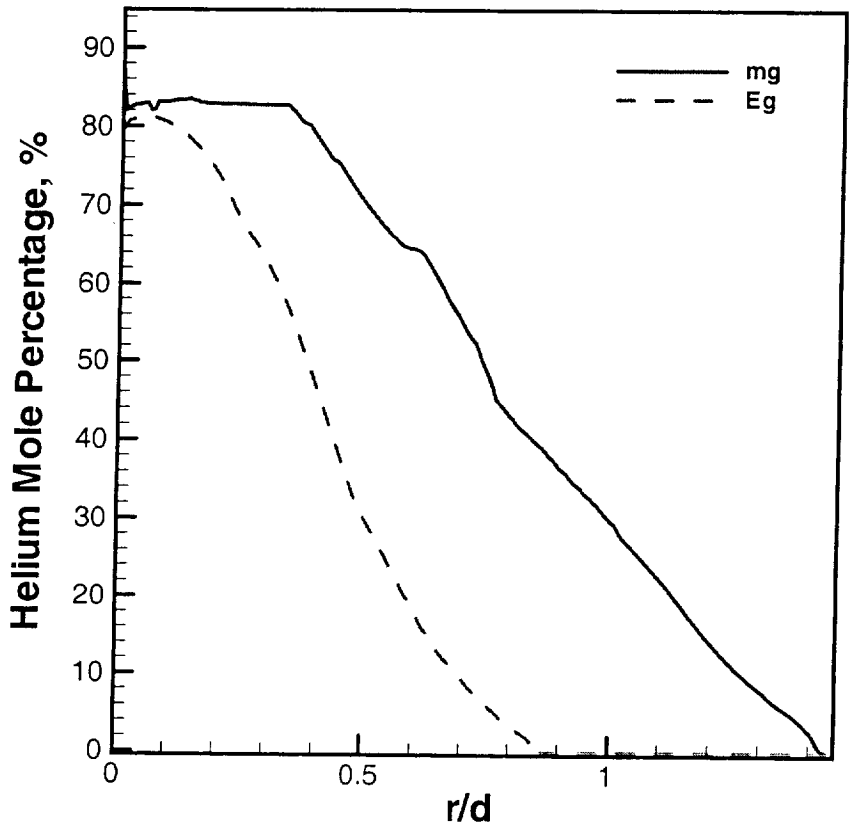

FIG. 8. Helium mole percentage in Earth gravity and microgravity at z/d = 1.5.

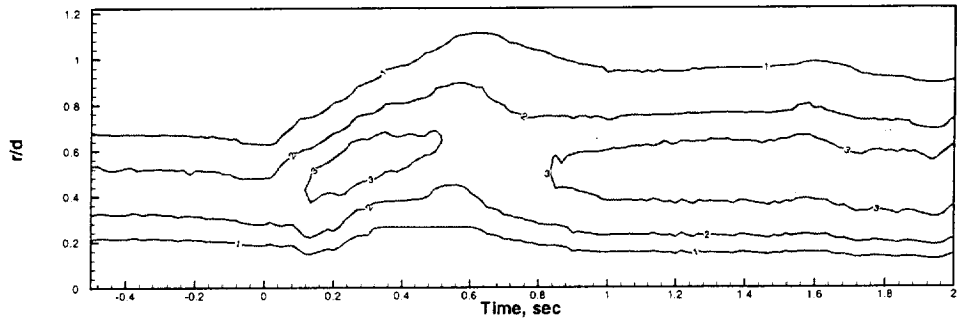

FIG. 9(a). Time traces of angular deflection in Earth gravity and microgravity at z/d = 1.5. Contour labels are 1:0.0002, 2:0.0003, and 3:0.0004 radians.

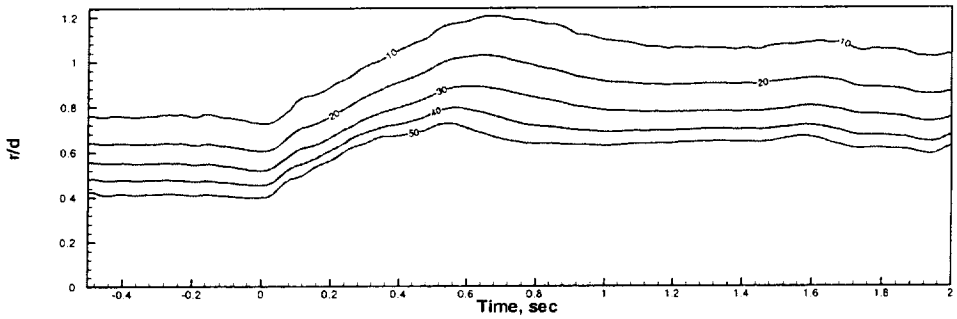

FIG. 9(b). Time traces of helium mole percentage in Earth gravity and microgravity at z/d = 1.5.

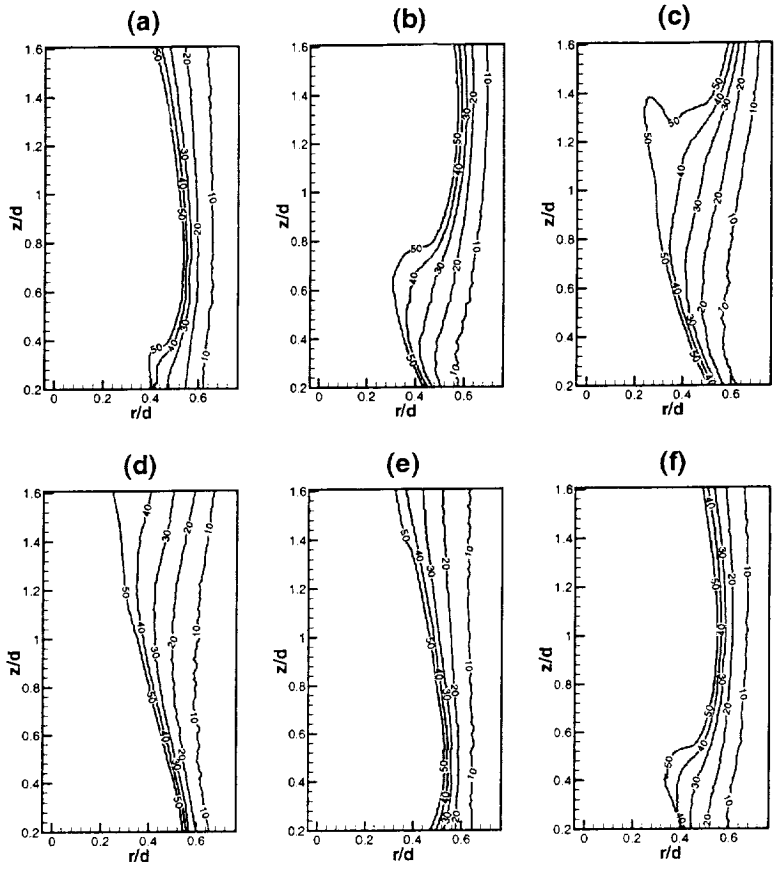

FIG. 10. Contours of helium mole percentage during a flicker cycle in Earth gravity.

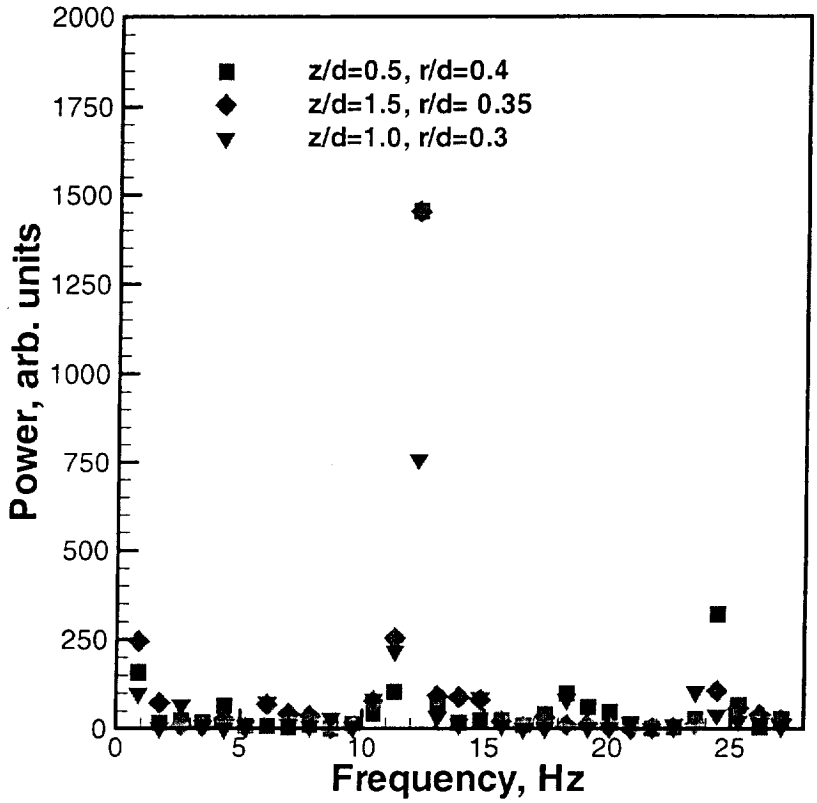

FIG. 11. Frequency power spectra density of oscillating jets in Earth gravity.

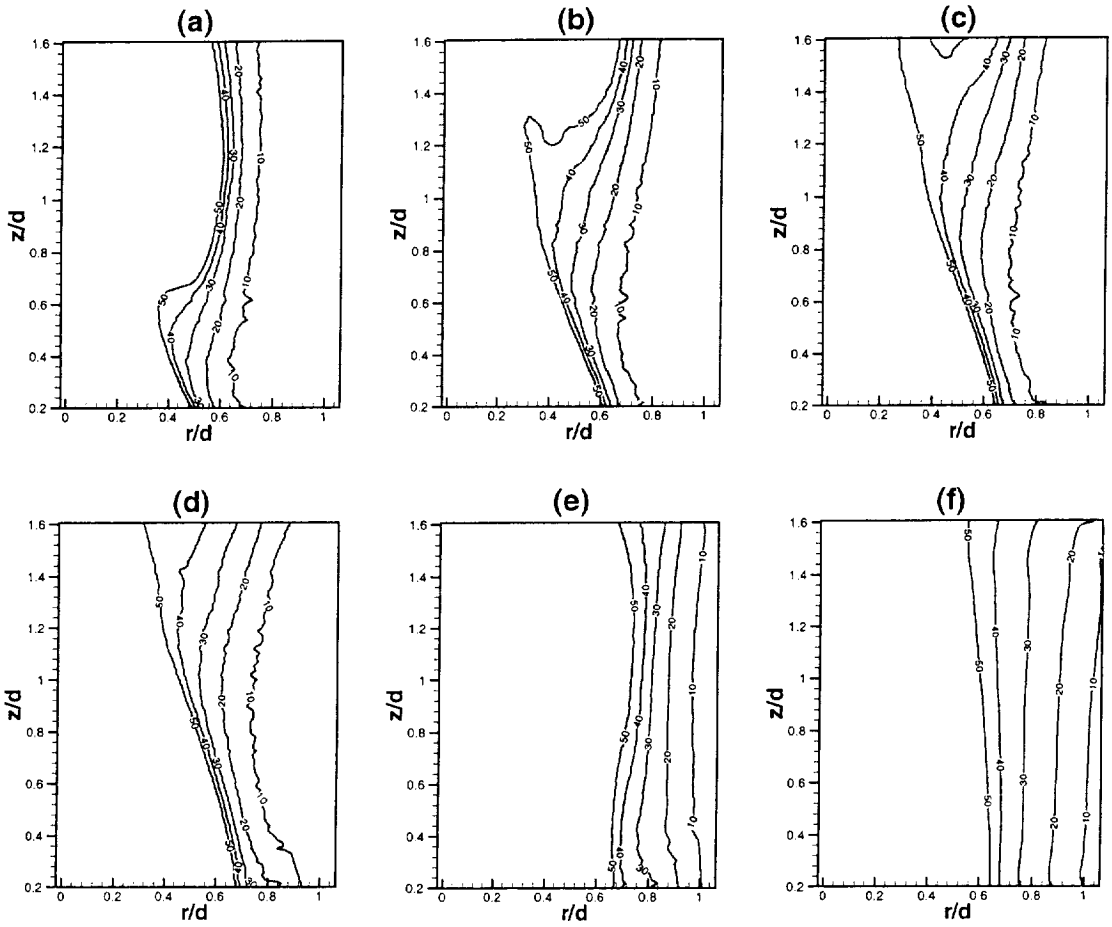

FIG. 12. Contours of helium mole percentage at: (a) t = 0 sec, (b) t = 1/60 sec, (c) t = 2/60 sec, (d) t= 3/60 sec, (e) t = 13/60, and (f) t = 2.0 sec.

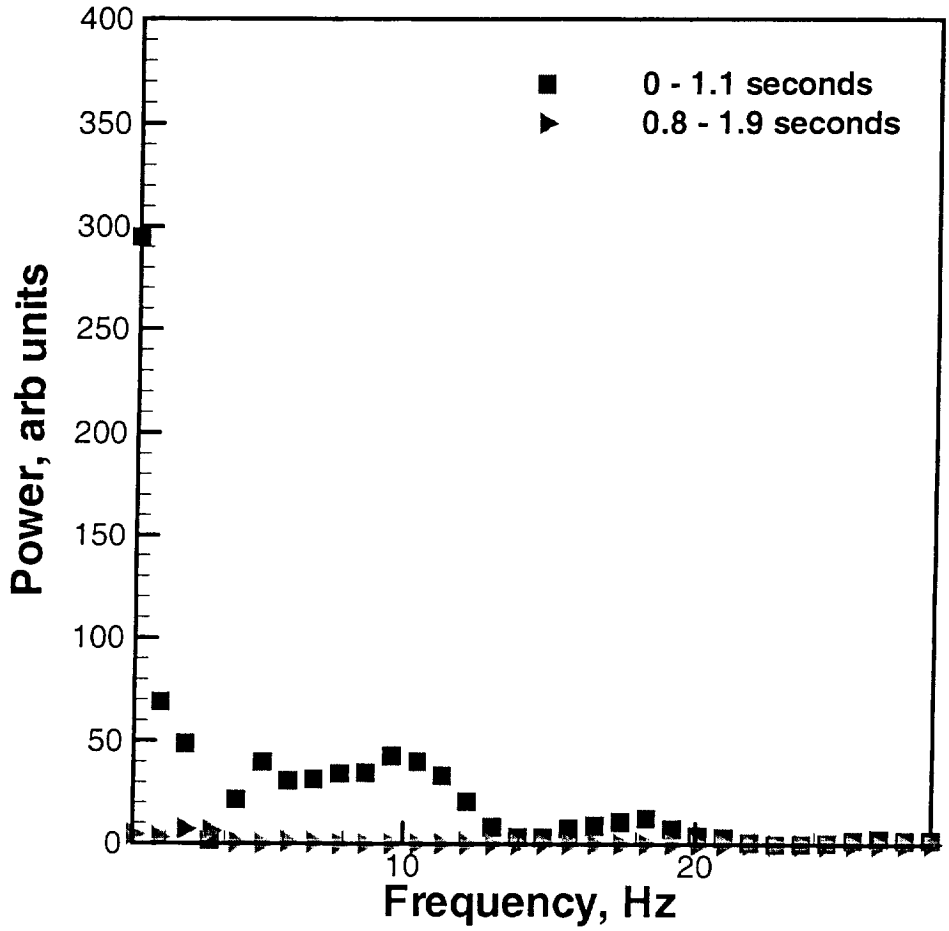

FIG. 13. Frequency power spectra density for two microgravity periods at z/d = 1.0, r/d = 0.6.

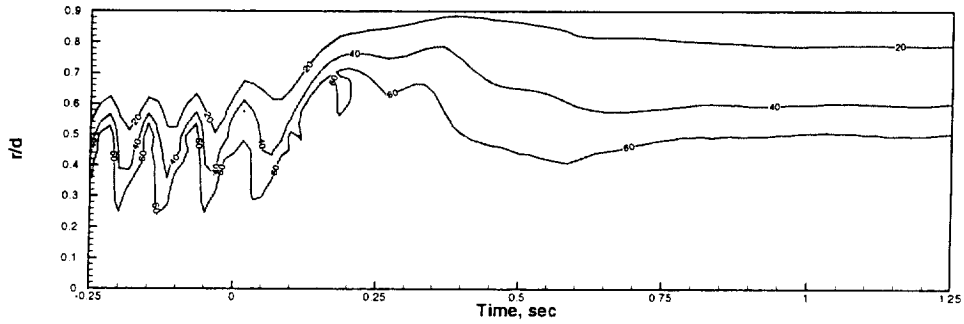

FIG. 14. Time traces of helium mole percentage in Earth gravity and microgravity at z/d = 1.0.

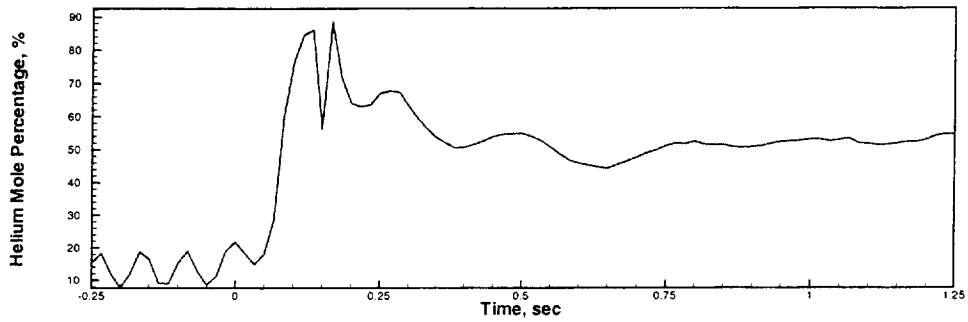

FIG. 15 (a). Helium mole percentage in Earth gravity and microgravity at z/d = 0.5, r/d = 0.6.

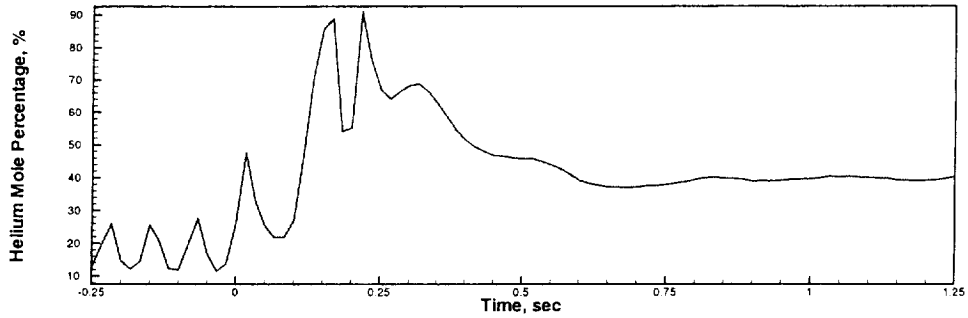

FIG. 15 (b). Helium mole percentage in Earth gravity and microgravity at z/d = 1, r/d = 0.6.

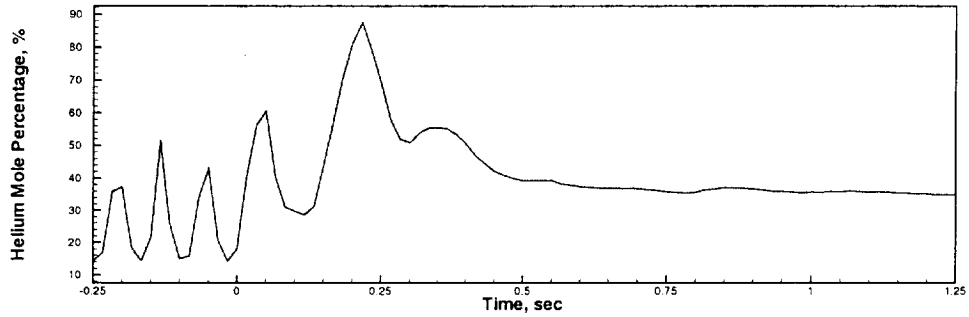

FIG. 15 (c). Helium mole percentage in Earth gravity and microgravity at z/d = 1.5, r/d = 0.6.